Introduction of a covalent histidine–heme linkage in a hemoglobin: A promising tool for heme protein engineering.

Selena L. Rice, Matthew R. Preimesberger, Eric A. Johnson, and Juliette T. J. Lecomte

Supporting Information

Table S1: Optical properties of WT, T111H, and L75H CtrHbs[a]

State/Protein[b]	WT CtrHb	T111H CtrHb	L75H CtrHb
ferric (this work)	409 (117)[c]	411 (117)	409 (117)
	535 (8.7)	531 (9.6)	530 (12)
ferric[d]	410 (110)		
	535 (8.5)		
cyanomet (this work)	416 (97.6)[e]	417 (114)	416 (119)
	546 (11)	545 (13)	544 (13)
cyanomet[e]	416 (97.6)		
	547 (11)		
ferrous (this work)	427 (98.3)	429 (96.8)	425 (111)
	529 (sh), 557 (13)	530 (sh), 559 (13)	529 (10), 558 (17)
ferrous[d]	426 (108)		
	529 (sh), 557 (15)		
ferrous cyanide (this work)[f]	431 (142)	430 (152)	n/a
	534 (14), 564 (21)	534 (15), 564 (22)	
ferrous cyanide[e]	434 (149)		
ferrous cyanide	n/a	428 (163)	426 (184)
(X-linked, this work)		530 (15), 561 (20)	530 (18), 561 (23)

[a] Data at pH 7.1, room temperature. Wavelength maxima are given in nm (extinction coefficients are in mM^{-1} cm^{-1}).

[b] For all three proteins, mass spectrometry data (Acquity / Xevo-G2 UPLC-MS, Waters) were consistent with the coded sequences from which the initial methionine had been cleaved. The experimental molecular masses were: WT CtrHb, 13297.7 Da (expected 13298.2 Da); L75H CtrHb, 13321.1 Da (expected 13322.2 Da); and T111H CtrHb (^{15}N labeled), 13491.7 Da (expected 13493.2 Da for 98% ^{15}N abundance). The WT CtrHb mass was unaffected by aerobic reduction with 2mM dithionite.

[c] Extinction coefficient calculated from the cyanomet value of 97.6 mM^{-1} cm^{-1} provided in [1]. The 117 mM^{-1} cm^{-1} value was applied to all three ferric CtrHbs. All other values calculated from the ferric state reference spectra.

[d] From [2], pH 7.5.

[e] From [1], pH 7.0, 20° C.

[f] The same spectrum with a Soret at 431 nm is obtained upon DT reduction of a cyanomet sample or addition of cyanide to a DT-reduced sample. This is in contrast to the observations published in [1].

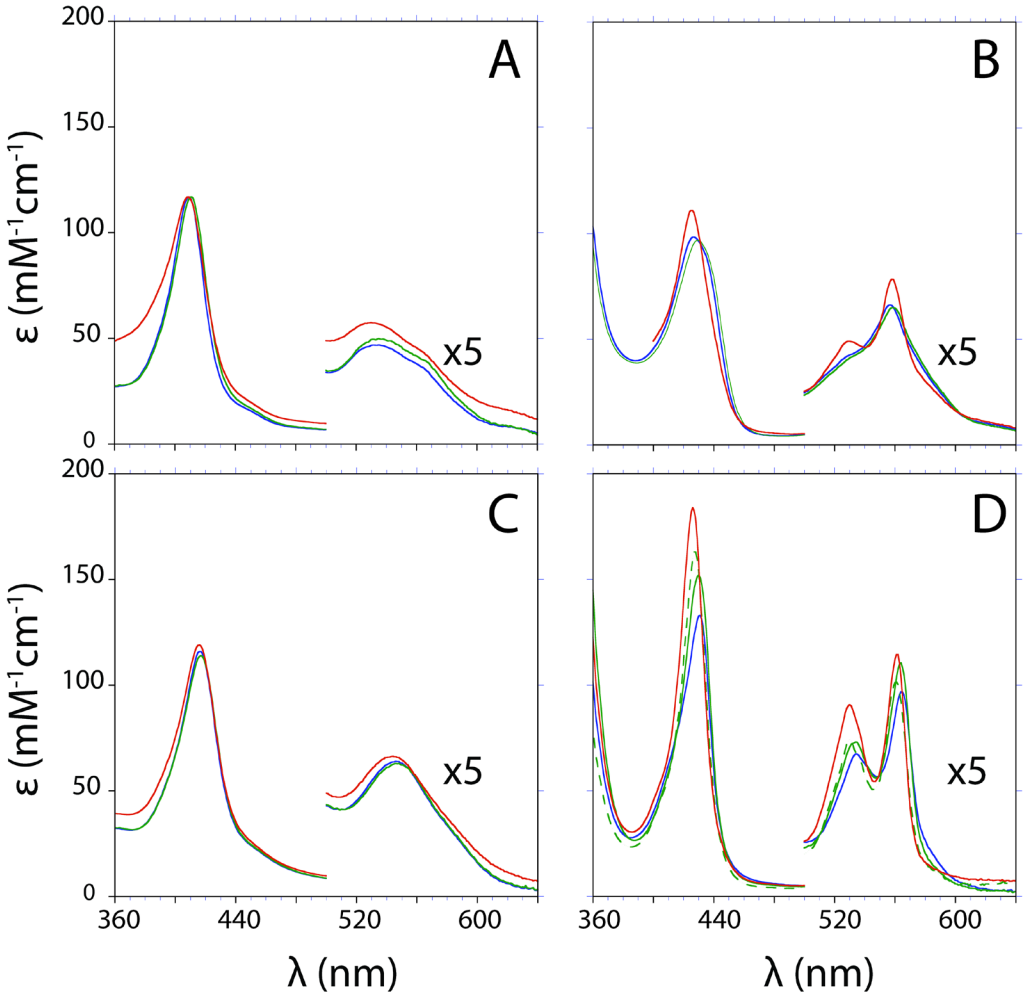

Figure S1: Reference optical spectra of WT (blue), T111H (green), and L75H (red) CtrHbs. All protein samples (4–10 μM) were prepared in 100 mM phosphate, pH ~7.1, and spectra were collected at room temperature. (A) Ferric state. The L75H variant exhibits some light scattering caused by aggregation. (B) Ferrous state. (C) Cyanomet state, prepared by addition of a 5-fold excess of KCN. (D) Ferrous cyanide-bound state prepared by DT reduction (~2 mM) of the cyanomet starting material. For T111H CtrHb, the solid line corresponds to the spectrum obtained initially after reduction; the dashed green line corresponds to the final product. Note the blue shift of the T111H and L75H variants relative to WT CtrHb.

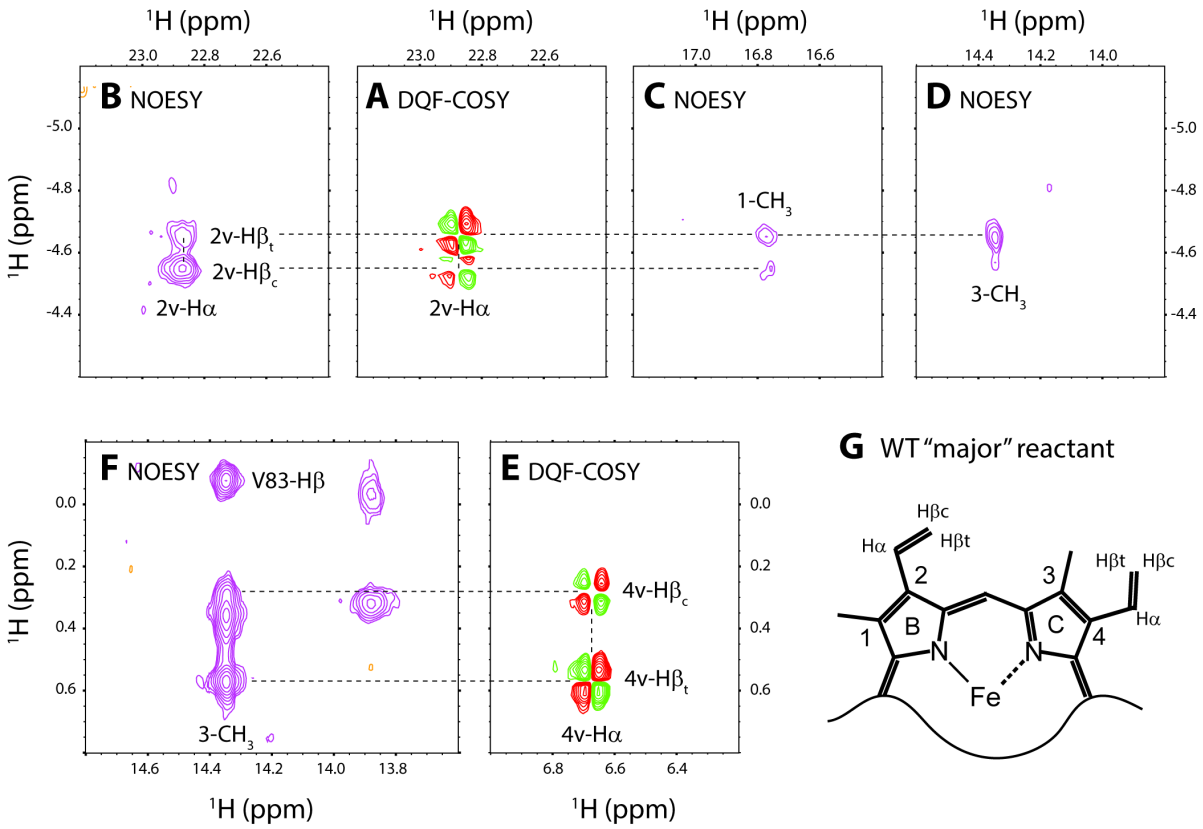

Figure S2: Portions of ^{1}H-^{1}H NOESY/DQF-COSY spectra for heme vinyl assignments in WT cyanomet CtrHb (major isomer) and vinyl orientation diagram. (A) *J*-coupled protons corresponding to the 2-vinyl group. (B) Intra-vinyl NOEs of the 2-vinyl group support 2-β_{cis} and 2-β_{trans} assignments. (C) The 2-vinyl β protons exhibit weak NOEs to the heme 1-CH_3. (D) The 2-vinyl β_{trans} proton is within dipolar contact with the heme 3-CH_3. Together, these connectivities support a *cis*-like orientation for the 2-vinyl group. (E) *J*-coupled protons corresponding to the 4-vinyl group. (F) The 4-vinyl β protons exhibit strong NOEs to the heme 3-CH_3 indicating it adopts a *trans*-like orientation. (G) Cartoon model depicting the orientations of vinyl groups within cyanomet WT CtrHb.

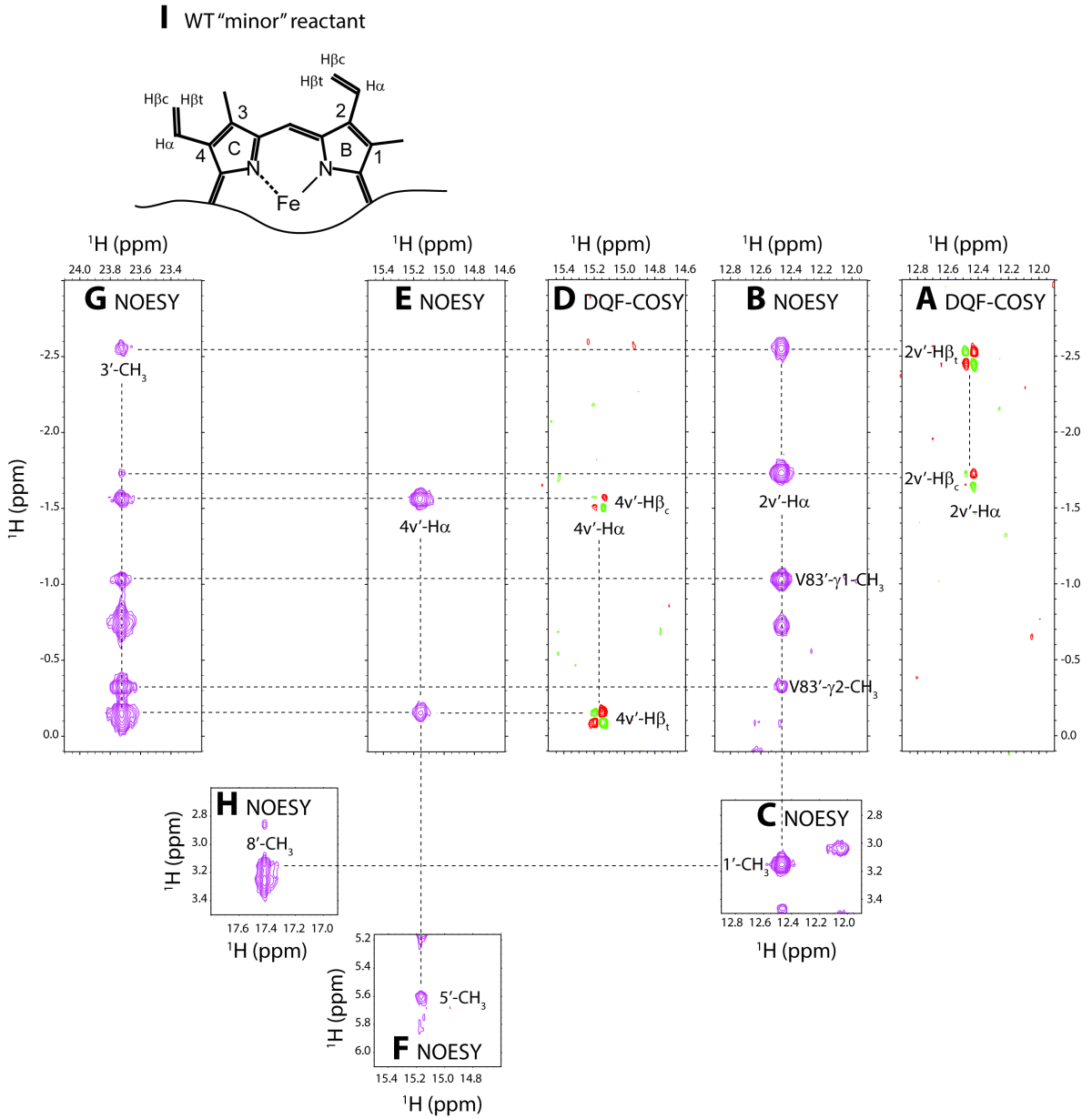

Figure S3: Portions of ^{1}H-^{1}H NOESY/DQF-COSY spectra for heme vinyl assignments in cyanomet WT CtrHb (minor isomer) and vinyl orientation diagram. (A) *J*-coupled protons assigned to the 2-vinyl group. (B) The 2-vinyl Hα has strong NOEs to the neighboring Hβs. (C) The 2-vinyl Hα also shows a strong contact to the heme 1-CH_3. (D) *J*-correlated signals assigned to the 4-vinyl group. (E) The 4-vinyl Hβs exhibit strong intra-vinyl NOE to the Hα. (F) The 4-vinyl Hα is in dipolar contact with the heme 5-CH_3. (G) The 2- and 4-vinyl Hβs are proximal to the heme 3-CH_3. (H) The heme 8-CH_3 shows an NOE to the 1-CH_3. The heme connectivity pattern is thus: 8-CH_3 ↔ 1-CH_3 ↔ 2-vinyl ↔ 3-CH_3 ↔ 4-vinyl ↔ 5-CH_3. (I) Cartoon model depicting vinyl orientations in cyanomet wild-type CtrHb.

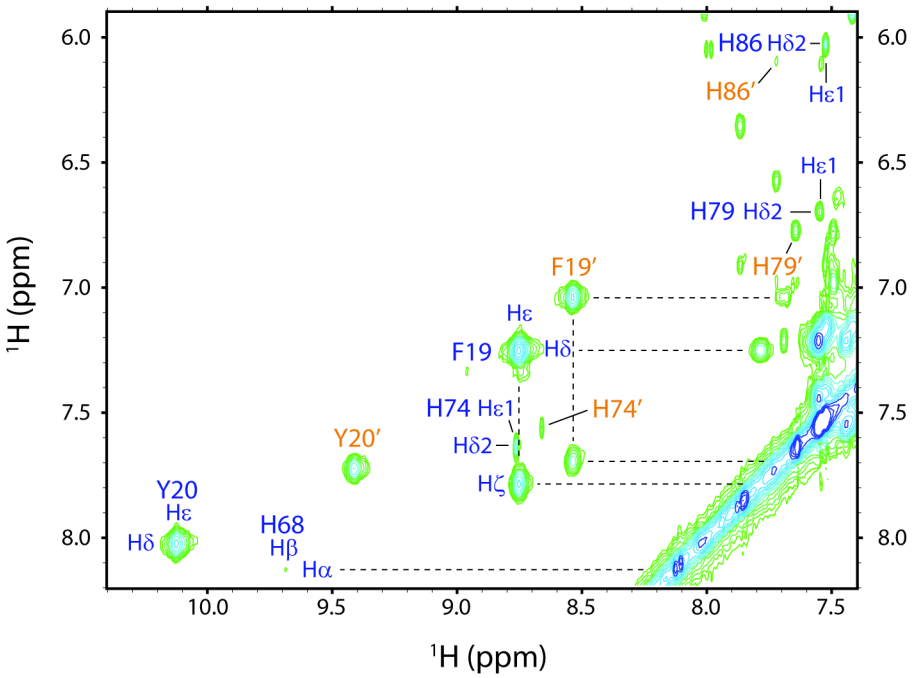

Figure S4: Downfield aromatic region of a ^{1}H-^{1}H TOCSY spectrum collected on cyanomet WT CtrHb. Assignments for some key heme pocket residues [H68 (His F8), Y20 (Tyr B10), and F19 (Phe B9)] and additional histidines are included. Peaks corresponding to the major heme orientational isomer are labeled in blue; peaks assigned to the minor heme orientational isomer are labeled in orange and denoted with prime.

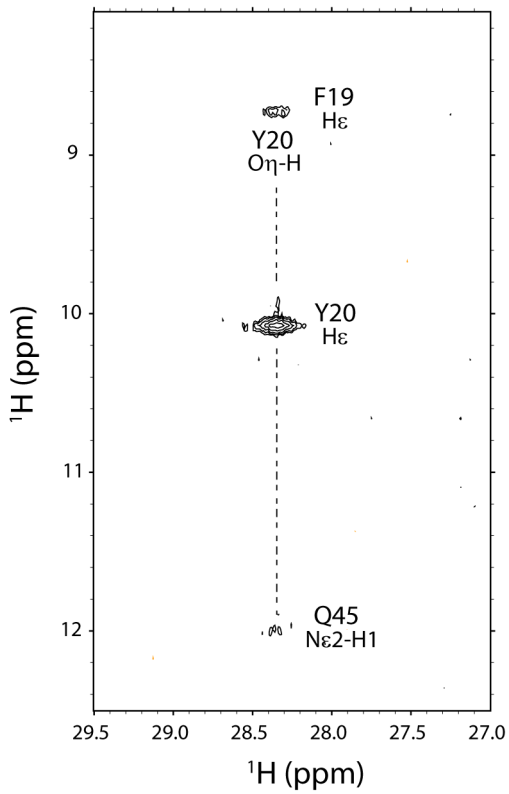

Figure S5: Key NOEs exhibited by the distal H-bonding Y20 OηH (Tyr B10) in cyanomet CtrHb. A downfield exchangeable proton (~28.4 ppm) is detected in WT NOESY data collected in H_2O. A strong NOE connects this signal to the Y20 CεHs. Weaker contacts to the distal residues F19 and Q45 are also observed. The NOEs, lability, and far downfield shift of the 28.4 ppm proton support its assignment to the distal Y20 OηH (Tyr B10), which stabilizes exogenous cyanide. Corresponding signals were observed for both cyanomet T111H and L75H CtrHb variants (see Figure 2, peaks labeled a), demonstrating that the variations did not appreciably perturb the distal cyanide H-bond network.

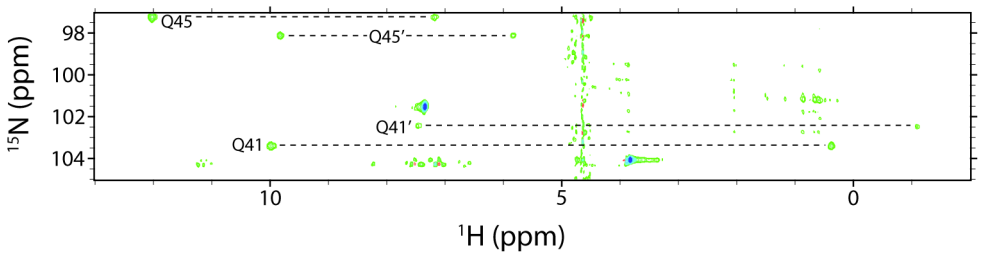

Figure S6: ^{1}H-^{15}N HSQC spectral region showing the highly shifted NH_2 systems of distal H-bonding Q41 and Q45 (Gln E7 and E11) residues. The highly shifted proton resonances of four NH_2 groups were tentatively assigned to the distal H-bonding residues Q45 and Q41 in the major and minor heme orientational isomers. The same signals are detected in both cyanomet T111H and L75H CtrHbs.

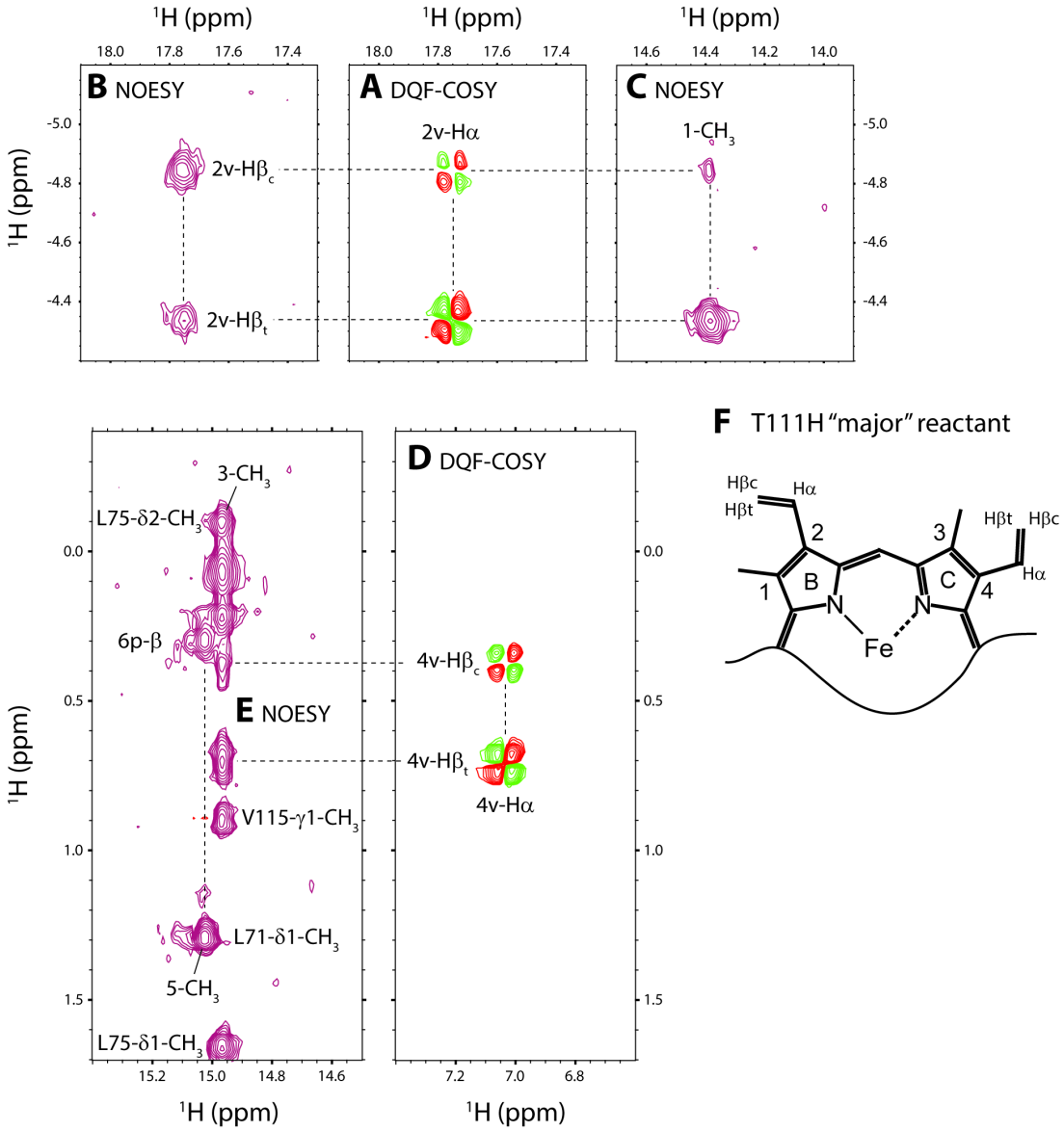

Figure S7: Portions of ^{1}H-^{1}H NOESY/DQF-COSY spectra for heme vinyl assignments in cyanomet T111H CtrHb (major isomer) and vinyl orientation diagram. (A) *J*-coupled AMX spin system assigned to the heme 2-vinyl group. (B) Intra-vinyl NOEs confirm the 2-β_{cis} and 2-β_{trans} proton assignments. (C) Strong NOE contacts between the 2-Hβs and the heme 1-CH_3 group orient the 2-vinyl in the *trans* conformation. These data support distinct 2-vinyl orientations between WT and T111H CtrHbs. (D) *J*-coupled signals corresponding to the heme 4-vinyl substituent. (E) NOEs between the 4-vinyl Hβs and the heme 3-CH_3 indicate that the former adopts a *trans* orientation, as observed for WT CtrHb. (F) Heme cartoon depicting the vinyl orientations consistent with NOE data.

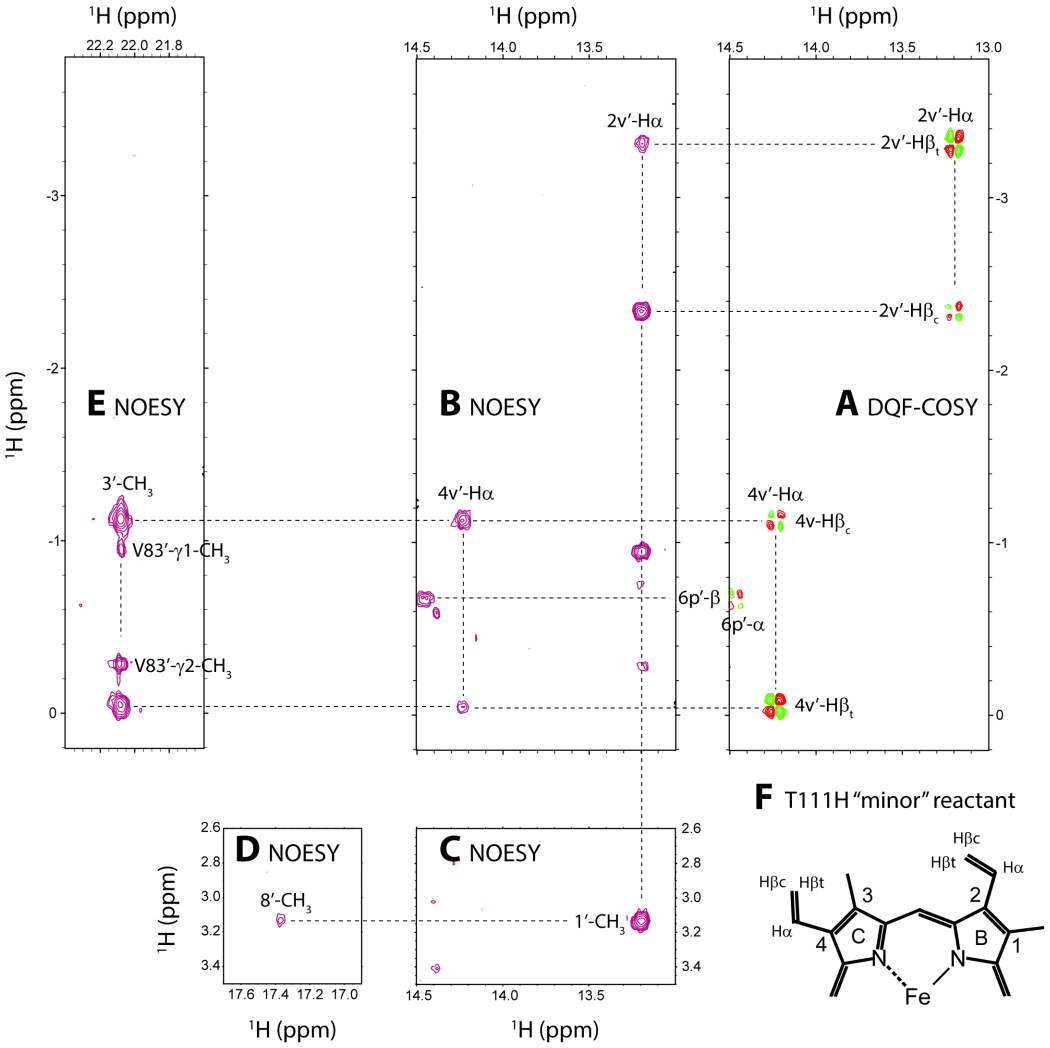

Figure S8: Portions of ^{1}H-^{1}H NOESY/DQF-COSY spectra for heme vinyl assignments in T111H cyanomet CtrHb (minor isomer) and vinyl orientation diagram. (A) *J*-correlated signals corresponding to the 2- and 4-vinyl groups. (B) Corresponding region displaying the intra-vinyl NOEs, confirming the assignment of β_{cis} and β_{trans} protons. (C) The 2-vinyl Hα displays a strong dipolar contact to the heme 1-CH_3 group supporting a 2-vinyl *cis* orientation. (D) A weak NOE was detected between the heme 1- and 8-CH_3. (E) The 4-vinyl β protons both show strong contacts to the heme 3-CH_3, indicative of the 4-vinyl group adopting a *trans* orientation. (F) Cartoon depiction of the heme vinyl group orientations.

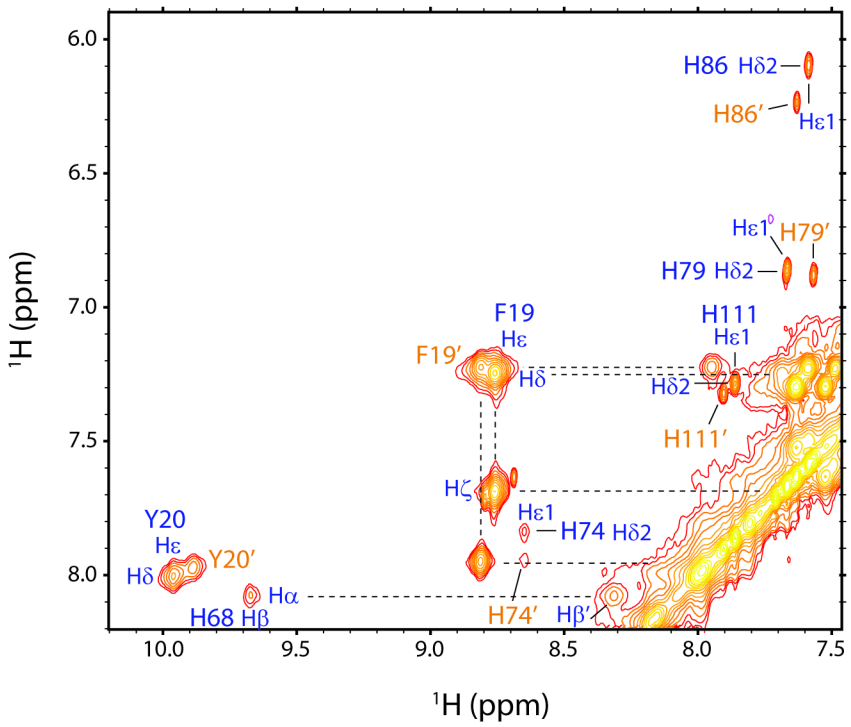

Figure S9: Downfield aromatic region of a ^{1}H-^{1}H TOCSY spectrum collected on cyanomet T111H CtrHb. Detectable histidine signals, along with distal heme pocket residues [Y20 (Tyr B10), F19 (Phe B9)] are labeled (major orientational isomer = blue, minor isomer = orange). Note the presence of the His111 Hε1 ↔ Hδ2 correlations. Interestingly, there is a closer chemical shift similarity between major and minor heme isomers in T111H CrHb compared to the WT CtrHb.

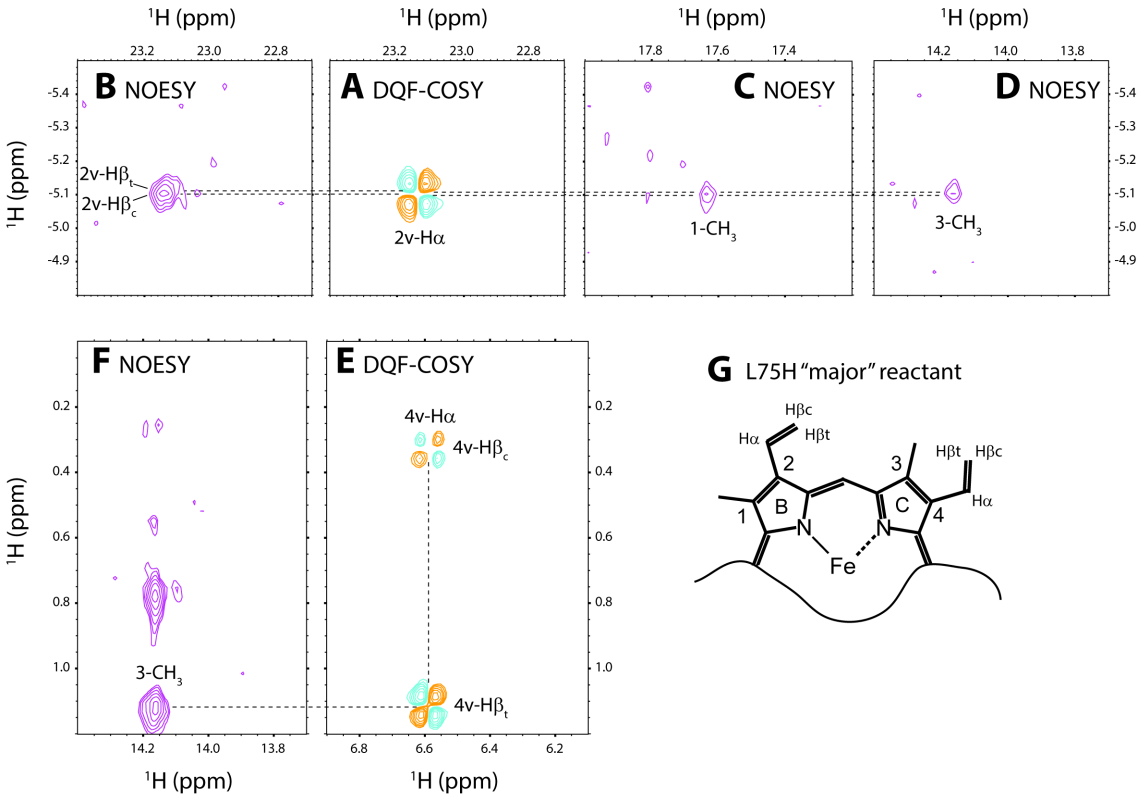

Figure S10: Portions of ^{1}H-^{1}H NOESY/DQF-COSY spectra for heme vinyl assignments in cyanomet L75H CtrHb (major isomer) and vinyl orientation diagram. (A) *J*-correlations exhibited between the 2-vinyl Hβs (overlapped) and the 2-vinyl Hα. (B) Corresponding region showing NOEs between the 2-vinyl Hβs and Hα. (C) The 2-vinyl Hβs are in weak dipolar contact with the heme 1-CH_3. (D) The 2-vinyl Hβs also show weak NOEs to the heme 3-CH_3 group, supporting a *cis* configuration. (E) DQF-COSY cross-peaks assigned to the heme 4-vinyl β_{cis}, β_{trans} and α protons. (F) The 4-vinyl Hβ_{trans} exhibits a strong NOE contact to the heme 3-CH_3 group, indicative of a 4-vinyl *trans* geometry. (G) Cartoon model showing the heme 2- and 4-vinyl orientations consistent with NMR data.

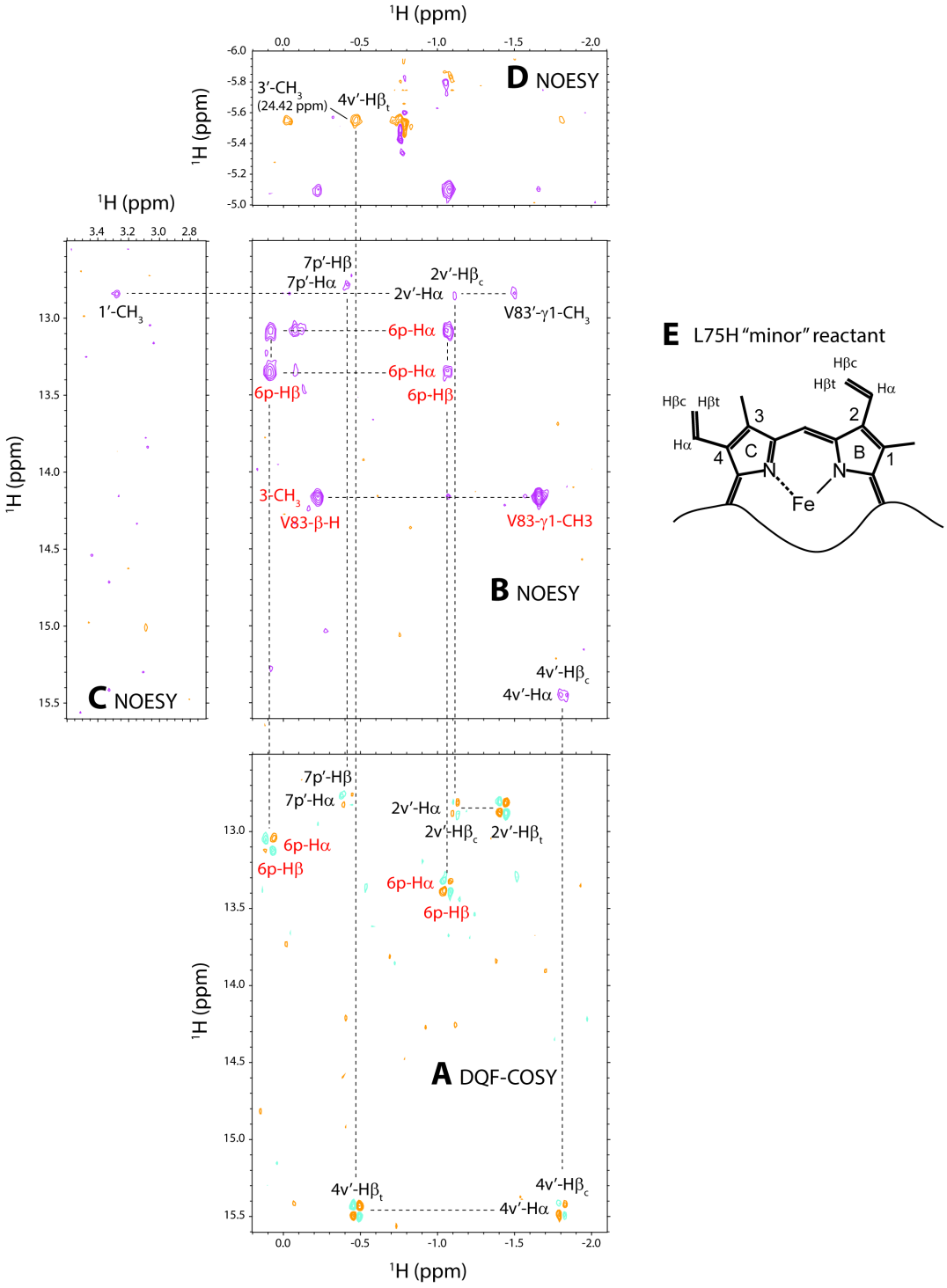

Figure S11: Portions of ^{1}H-^{1}H NOESY/DQF-COSY spectra for heme vinyl assignments in L75H cyanomet CtrHb (minor isomer) and vinyl orientation diagram. (A) *J*-correlations between the α and β protons of the heme 2- and 4-vinyl groups (black labels). Signals annotated with red labels derive from the L75H cyanomet CtrHb major heme isomer. (B) Corresponding region of the NOESY spectrum, highlighting intra-heme vinyl NOEs (labels as in A). (C) The 2-vinyl Hα exhibits a dipolar contact to

the heme 1-methyl. Because the Hβs do not show such effects, the data support a 2-vinyl *cis* orientation. (D) The 4-vinyl β_{trans} proton shows a strong NOE to the heme 3-CH_3 (folded). This strong contact defines a 4-vinyl *trans* orientation. (E) Heme structural model depicting vinyl orientations consistent with NOE data.

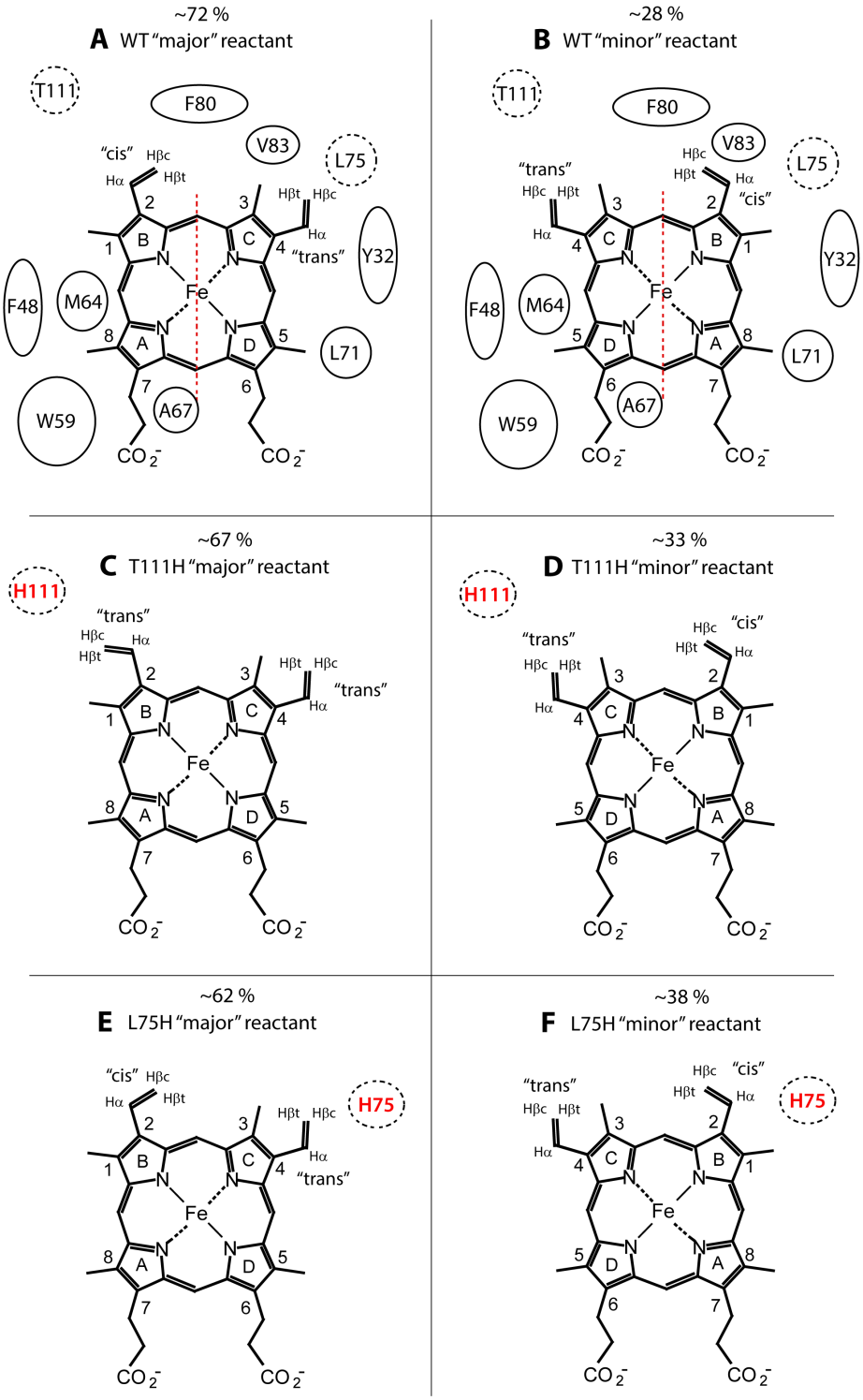

Figure S12: Structural summary of heme orientational isomers in wild-type (A, B), T111H (C, D), and L75H (E, F) cyanomet CtrHbs. The relative populations of each isomer, as estimated from integration of resolved ^{1}H 1D peak, are given in percent. These populations did not change appreciably over the course of data collection indicating extremely slow exchange. For the WT CtrHb major and minor

isomers (top row), several residues in proximity to the heme are depicted as ellipses. Within the left column (major heme isomers), the T111H variant displays a distinct heme 2-vinyl orientation with respect to WT and L75H CtrHbs. The minor heme isomers (right column) all displayed similar intra-heme NOEs, which supports a common vinyl configuration. In each depiction, the proximal histidine is above the page toward the reader.

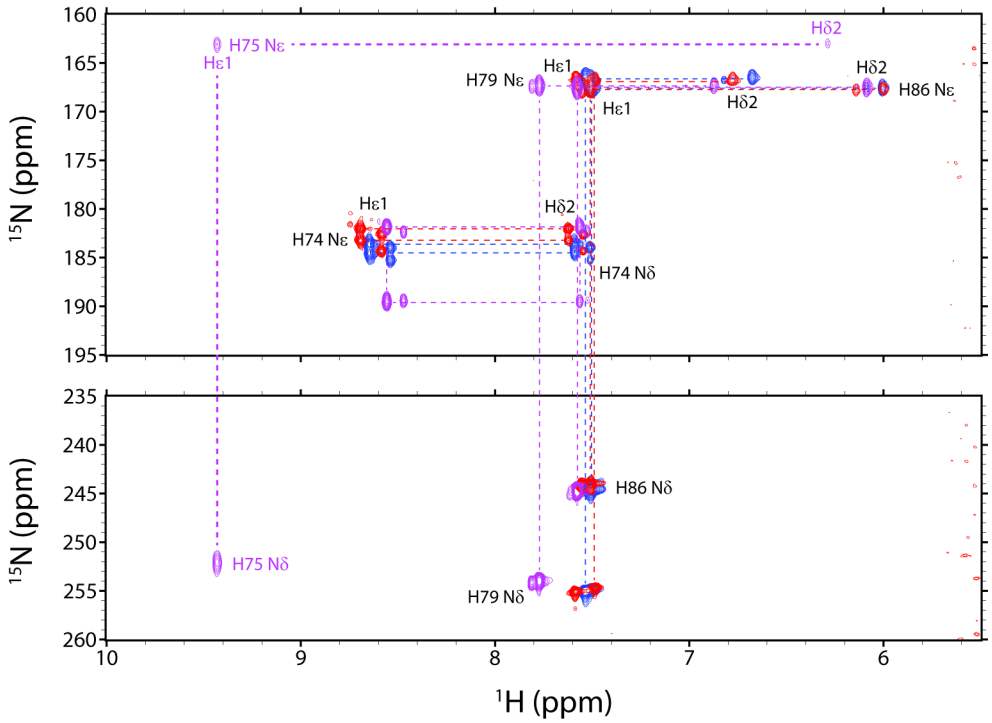

Figure S13: ^{1}H-^{15}N long-range HMQC ($1/2J_{NH}$ ~ 22 ms) spectral overlay of WT, T111H, and L75H cyanomet CtrHbs. All non-proximal histidine residues (H74, H79, and H86) are assignable in cyanomet WT CtrHb (blue peaks, black labels). For the T111H variant (red peaks), resonances corresponding to H74, H79, and H86 overlay well with the wild-type, but additional signals corresponding to H111 are not observed, likely because of exchange broadening. On the other hand, the L75H variant (magenta peaks) exhibits a new, highly shifted set of resonances attributable to H75 (magenta labels), in addition to minimally perturbed H74, H79, and H86 signals. The unusual chemical shifts observed for H75 protons are consistent with its close proximity to the paramagnetic (S = 1/2) heme.

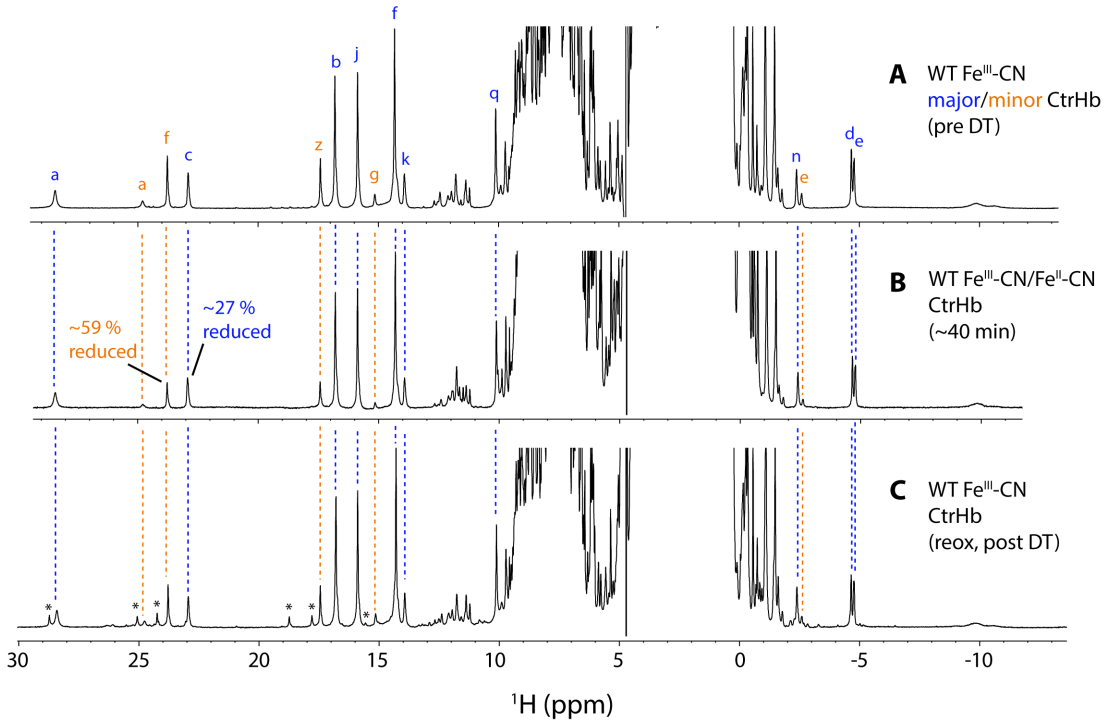

Figure S14: ^{1}H NMR spectra monitoring DT reduction of cyanide bound WT CtrHb (^{15}N amide decoupled). (A) Cyanomet (Fe^{III}-CN) ^{15}N-labeled protein spectrum prior to DT reduction. Assignments for select heme and protein ^{1}H signals are included. Peaks are labeled as in Figure 2 of the main text: a, Tyr20 OηH; b, heme 1-CH_3; c, heme 2-vinyl Hα; d, e, heme 2-vinyl Hβ_{cis}, Hβ_{trans}; f, heme 3-CH_3; g, heme 4-vinyl Hα; j, heme 5-CH_3; k, heme 6-propionate Hα, Hα'; n, heme 7-propionate Hβ; q, Tyr20 CεHs; z, heme 8-CH_3. The major heme orientational isomer (blue labels) occurs at a ~2.6:1 ratio over the minor isomer (orange labels). (B) Mixture of cyanomet (Fe^{III}-CN, paramagnetic) and ferrous cyanide (Fe^{II}-CN, diamagnetic) proteins ~40 min following reduction with 6 mM DT. The dashed lines connect remaining cyanomet signals. Assuming no damage occurred to the protein, the decrease in cyanomet peak intensities indicates that approximately 27% of the major isomer was reduced. Interestingly, the minor isomer displays increased susceptibility to reduction (~59% reduced), suggesting that the major and minor heme orientational isomers differ in their ability to stabilize exogenous cyanide in the ferrous state. (C) Following ~6 h DT reduction, the sample was completely reoxidized. The predominant forms detected were identical to those observed prior to reduction indicating minimal reaction (dashed lines). However, an additional minor species is detected (asterisks) in an indication of heme side reaction. A–C. Sample conditions: pH ~7.1, 10 % D_2O, 298 K.

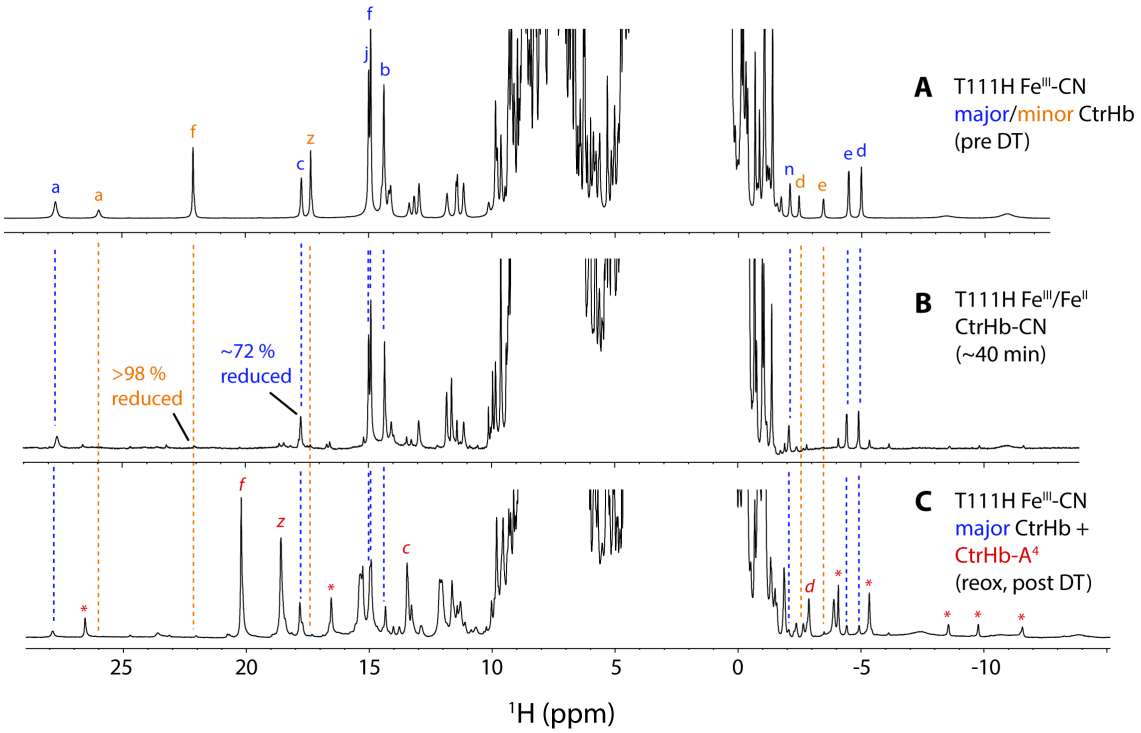

Figure S15: ^{1}H NMR spectra following DT reduction of cyanide bound T111H CtrHb. (A) Cyanomet (Fe^{III}-CN) protein spectrum before DT reduction. Assignments for select heme and protein ^{1}H signals are included. Peaks are labeled as in Figure 2 of the main text: a, Tyr20 OηH; b, heme 1-CH_3; c, heme 2-vinyl Hα; d, e, heme 2-vinyl $H\beta_{cis}$, $H\beta_{trans}$; f, heme 3-CH_3; j, heme 5-CH_3; n, heme 7-propionate Hβ; z, heme 8-CH_3. The major heme orientational isomer (blue labels) occurs at a ~2:1 ratio over the minor isomer (orange labels). (B) Mixture of cyanomet (Fe^{III}-CN, paramagnetic) and ferrous cyanide (Fe^{II}-CN, diamagnetic) T111H proteins ~40 min following reduction with 6 mM DT. The dashed lines connect remaining cyanomet signals. Under the assumption of no protein damage, the decrease in cyanomet peak intensities indicates that approximately 72% of the major isomer was reduced. In contrast, virtually none of the cyanomet minor isomer remains. Therefore, as in WT CtrHb, the T111H minor heme orientational isomer displays an enhanced susceptibility to DT reduction when compared to the major isomer. However, both isomers of T111H CtrHb are reduced more readily than WT CtrHb. (C) Following ~7 h DT reduction, the sample was completely reoxidized. The predominant form (~60%, red labels) corresponds to the major reaction product (cyanomet T111H CtrHb-A^4). Additionally, the unreacted major isomer is observed (blue dashed lines). At least one other form (red asterisks) is noted. This form was not studied further, but we note that the shifts do not suggest formation of T111H CtrHb-A^2. Sample conditions: pH ~7.1, 10 % D_2O, 298 K.

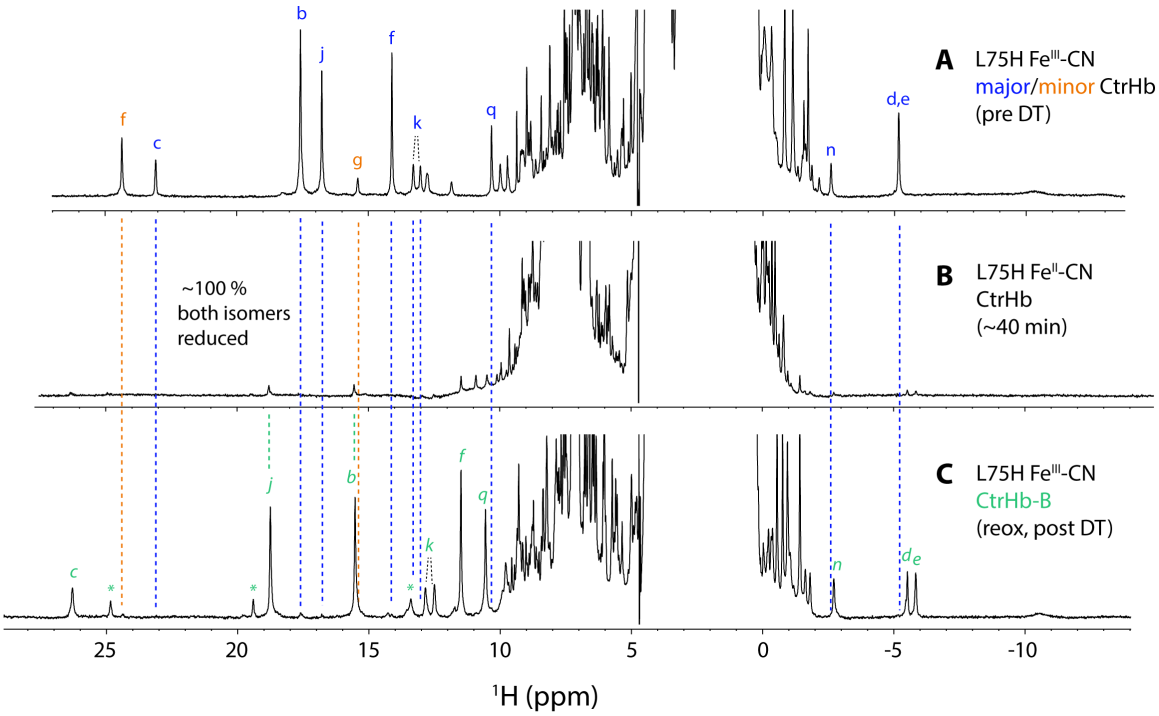

Figure S16: ^{1}H NMR spectra following DT reduction of cyanide bound L75H CtrHb. (A) Cyanomet (Fe^{III}-CN) protein spectrum prior to DT reduction (100% D_2O, pH* = 7.4). Assignments for select heme and protein ^{1}H signals are included. Peaks are labeled as in Figure 2 of the main text: a, Tyr20 OηH; b, heme 1-CH_3; c, heme 2-vinyl Hα; d, e, heme 2-vinyl $H\beta_{cis}$, $H\beta_{trans}$; f, heme 3-CH_3; g, heme 4-vinyl Hα; j, heme 5-CH_3; k, heme 6-propionate Hα, Hα'; n, heme 7-propionate Hβ; q, Tyr20 CεHs; z, heme 8-CH_3. The major heme orientational isomer (blue labels) occurs at a ~3:2 ratio over the minor isomer (orange labels). (B) The sample was exchanged into H_2O (pH 7.3) and reduced with ~8 mM dithionite. After ~40 min, the sample contained no detectable resonances attributable to either the major or minor cyanomet reactants. Thus, unlike both T111H and WT cyanomet CtrHbs, the L75H variant is completely reduced to the ferrous cyanide bound form. (C) Following ~2 h DT reduction, the sample was completely reoxidized and exchanged back into D_2O (pH* 7.2). Both major and minor isomer reactant resonances had essentially vanished (orange and blue dashed lines) but a new set of resonances, corresponding to > 90% of the sample was observed and attributed to the primary product: L75H cyanomet CtrHb-B (cyan labels). A minor product (< 10%, cyan asterisks) was also detected but not examined in this work. Preliminary evidence (lr-HMQC) suggests the minor product in L75H is H75 Nε2–2-Cα linkage. All data were collected at 298 K.

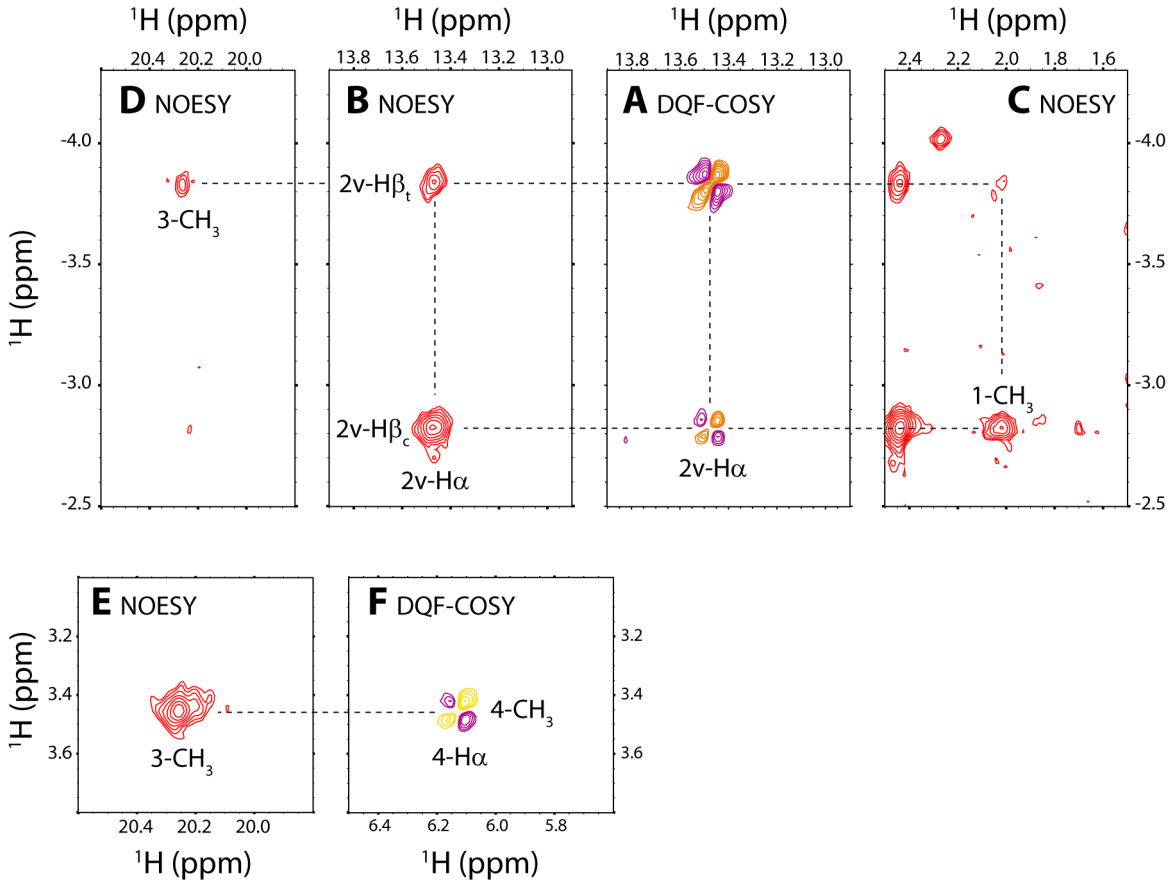

Figure S17: Portions of ^{1}H-^{1}H NOESY/DQF-COSY spectra for heme assignments in cyanomet T111H CtrHb-A[4] (covalent adduct). (A) *J*-correlated resonances assigned to the 2-vinyl Hα and Hβs. (B) Corresponding region showing NOEs in support of the 2-vinyl $H\beta_{cis}$ and $H\beta_{trans}$ assignments. (C) The 2-vinyl $H\beta_{cis}$ is in dipolar contact with the heme 1-CH_3. (D) The 2-vinyl $H\beta_{trans}$ displays an NOE to the heme 3-CH_3. Together, these data support a *cis* or "twist" configuration for the 2-vinyl group. No additional vinyl group was detected. (E) The 3-CH_3, which typically displays NOEs to the heme 4-vinyl, instead showed a strong contact with a methyl group (~3.4 ppm), in agreement with a modification at the heme 4-substituent. (F) The tentative 4-heme methyl group displayed a *J*-correlation to a signal at (~6.1 ppm), suggesting the modification of the vinyl $C\alpha H{=}C\beta H_2$ group into a $C\alpha H$-$C\beta H_3$ substituent.

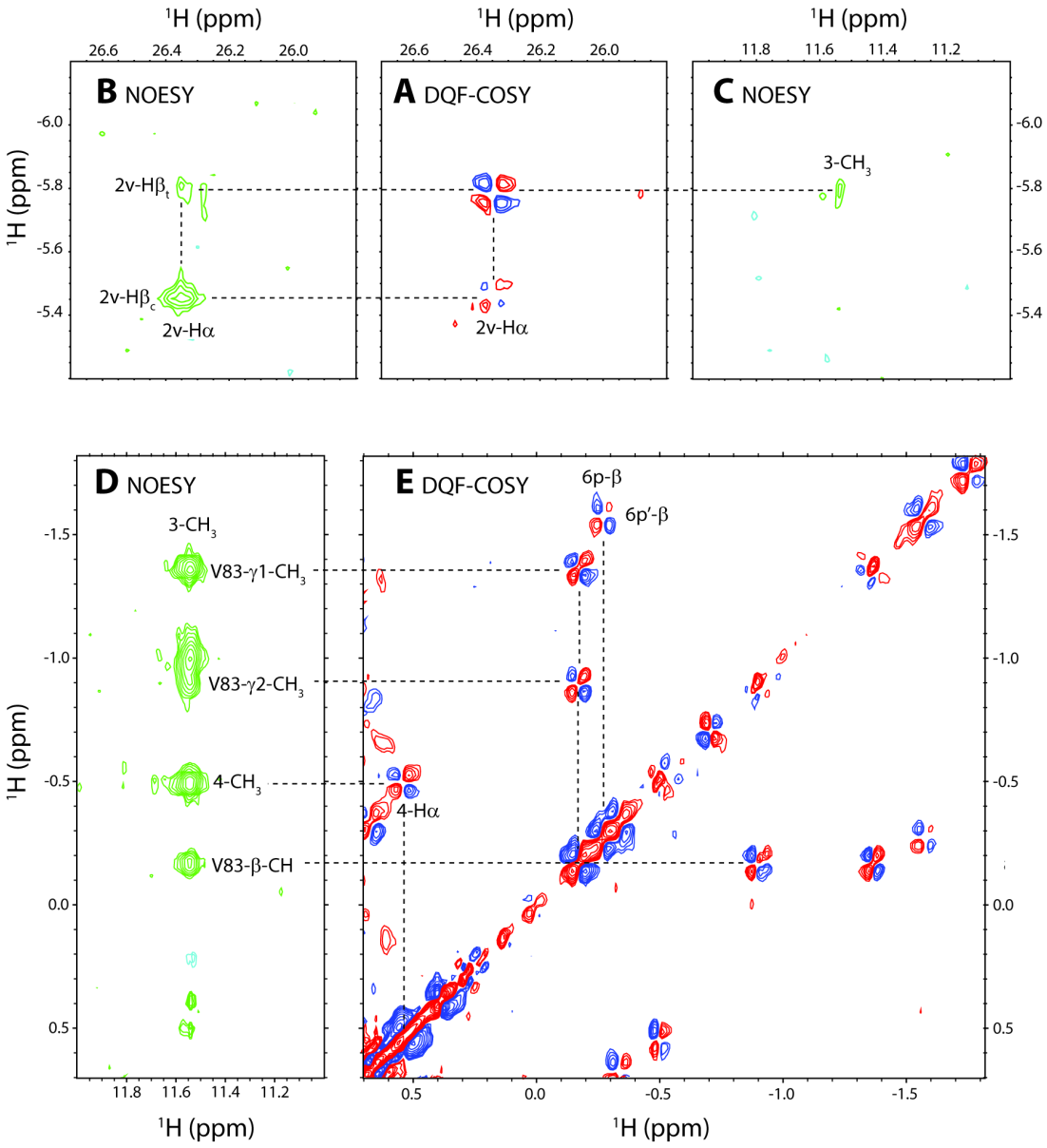

Figure S18: Portions of ^{1}H-^{1}H NOESY/DQF-COSY spectra for heme assignments in L75H cyanomet CtrHb-B (covalent product). (A) *J*-correlations exhibited between 2-vinyl protons. (B) Corresponding region showing NOEs in support of 2-vinyl Hβ_{cis} and Hβ_{trans} assignments. (C) The 2-vinyl Hβ_{trans} displays a weak NOE to the heme 3-CH_3. The intra-heme connectivities are consistent with the 2-vinyl group adopting a *cis* or "twist" orientation. (D) The upfield methyl protons (–0.5 ppm) *J*-correlated to His75 in the ^{15}N histidine-selective lr-HMQC spectrum (Figure 5, main text) displays a strong NOE to the heme 3-CH_3. This contact, along with the absence of a second vinyl system in DQF-COSY data, indicates that the 4-substituent has undergone modification. (E) The heme 4-CβH_3 displays a single *J*-correlation assigned to the heme 4-CαH.

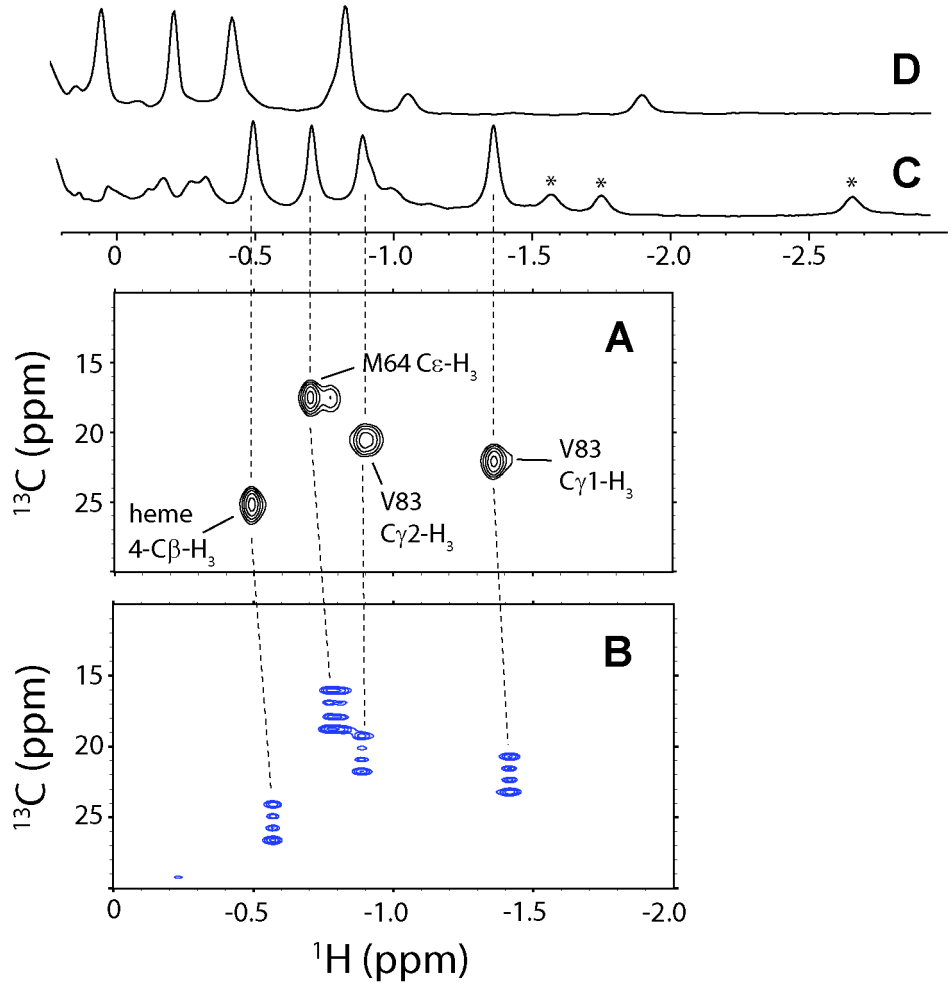

Figure S19: Identification of the resolved peak at a ^{1}H shift of –0.49 ppm as a methyl group. (A) The ^{1}H-^{13}C HMQC data shown in Fig. 6. (B) The corresponding coupled ^{1}H-^{13}C HSQC data clearly showing a 3:1:1:3 quartet at –0.49 ppm. (C) The ^{1}H 1D data at 298 K. (D) The ^{1}H 1D data at 313 K. The region shown contains the methyl groups of Val83 and Met64. All four methyl groups are highly sensitive to temperature (Curie effect) as illustrated in (D). (A) and (B) were collected on different samples and different spectrometers. Slight changes in temperature and pH explain the small shifts in the proton dimension. For comparison, the peaks marked with asterisks correspond to heme propionate signals with single proton intensity.

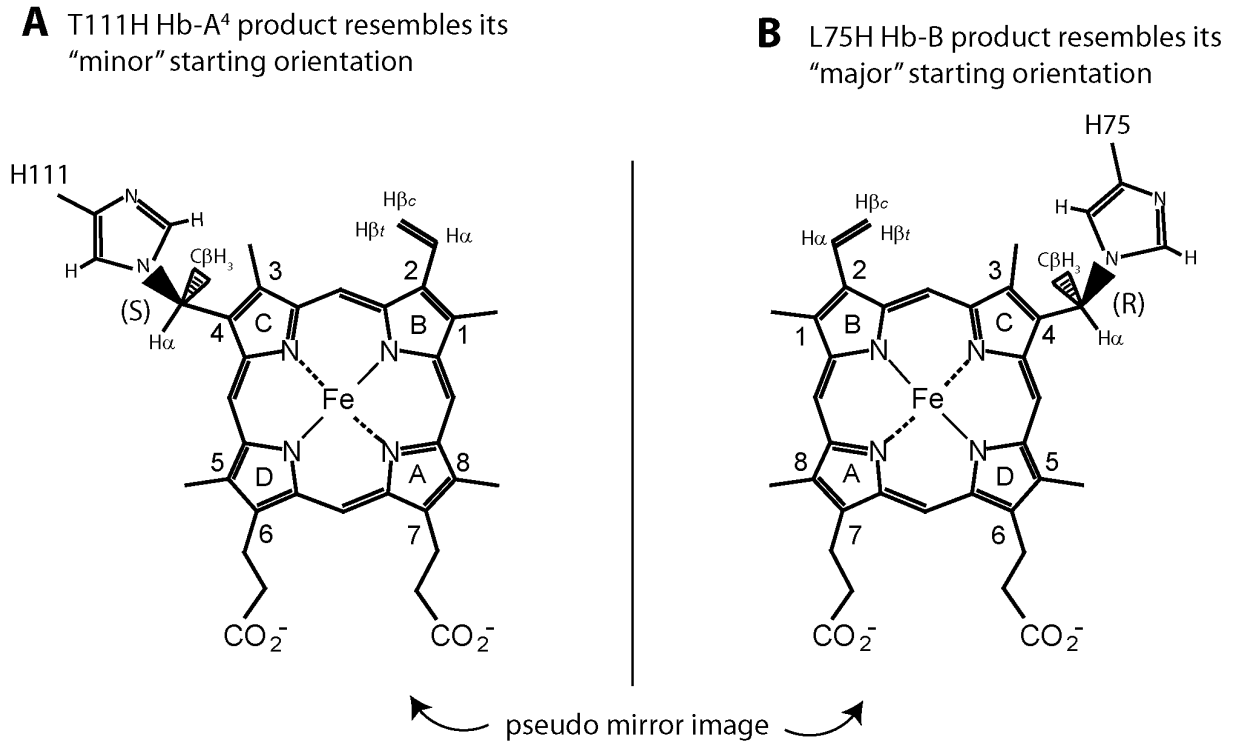

Figure S20: Proposed structures of the histidine-heme modifications in (A) T111H CtrHb-A[4] and (B) L75H CtrHb-B. The T111H product is tentative as no long-range coupling was observed between the modified His111 Nε and the heme. However, NOEs between the His111 Hδ2 and Hε1 are consistent with the orientation depicted. With regards to the L75H product, the long-range ^{15}Nε2-CβH$_3$ *J*-correlation establishes that modification occurred at His75 Nε2. Since a methyl group was detected at the 4-substituent, a Nε2-Cα– CβH$_3$ His-heme linkage can be inferred. As shown, the model is consistent with NOEs observed between the modified H75 side chain and covalently bound heme.

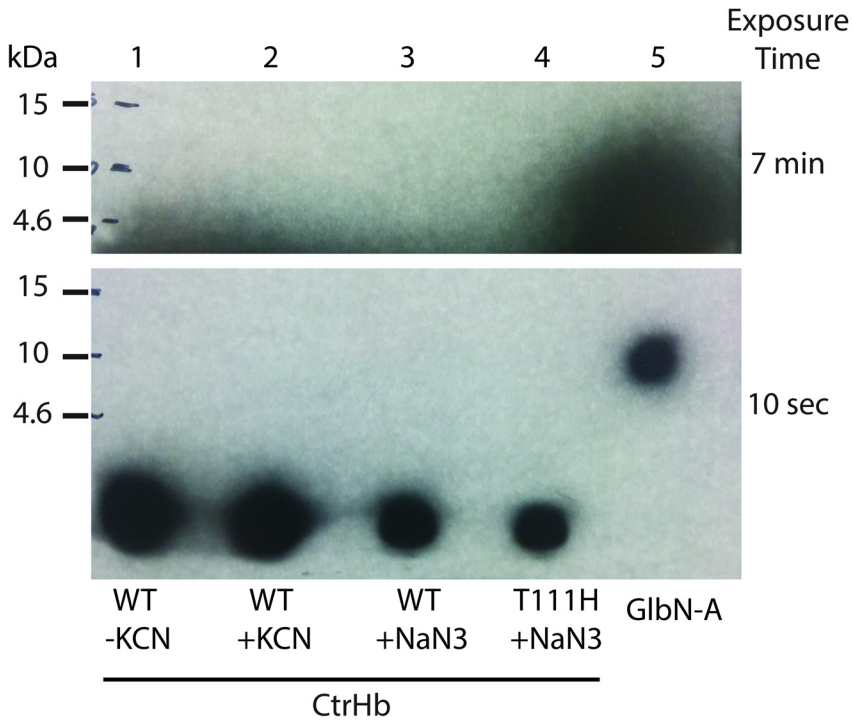

Figure S21: ECL SDS-PAGE showing no heme attachment in T111H CtrHb when azide is used in place of cyanide. Five-fold excess KCN (+KCN) or 10 mM NaN_3 (+NaN_3) was added to the ferric form of the designated protein and incubated for 20 min. Subsequently, 2 mM DT was added to each sample and incubated for 3 h at RT, followed by passage over a ~1.3 cm^3 DEAE column. The figure shows film that was exposed for either 10 s or 7 min. As expected, all of the WT CrtHb samples (lanes 1–3) showed the heme migrating with the dye front. The T111H CtrHb +NaN_3 sample (lane 4) also showed heme only migrating with the dye front. No crosslinked heme was detected in this sample even after the 7 min exposure. To account for possible inhibition of peroxidase activity by azide, a sample of the more reactive L75H CtrHb was treated with azide/DT, then purified by DEAE chromatography. The protein lost heme on the column. This demonstrates that, unlike cyanide, azide does not facilitate crosslink formation in T111H or L75H CtrHb. Crosslinked GlbN (GlbN-A, lane 5) was used as a control.

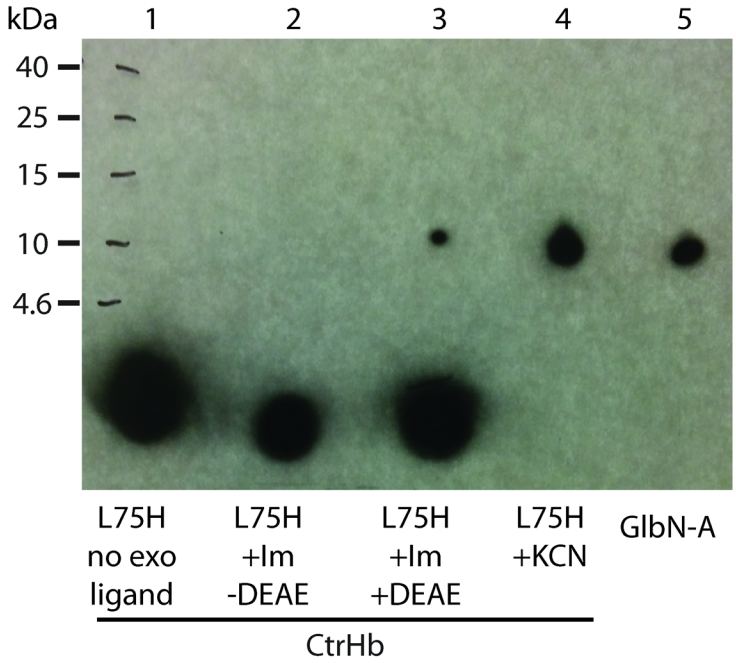

Figure S22: ECL SDS-PAGE demonstrating partial modification of L75H CtrHb when imidazole is used instead of cyanide. Ten-fold excess imidazole (+Im) or 5-fold excess KCN (+KCN) was added to L75H and incubated for at least 4 h or 20 min with imidazole or cyanide, respectively. All L75H CtrHb samples, except the L75H CtrHb sample to which no exogenous ligand was added (lane 1), were subsequently reduced with 2 mM DT for 3 h. The L75H CtrHb +Im/-DEAE sample in lane 2 does not show heme migrating with the protein. However, this sample was not passed over a DEAE column to strip some of the imidazole from the heme. Thus, when compared to the L75H CtrHb +Im/+DEAE sample (lane 3) that was cleaned by passage through a short DEAE column, imidazole is shown to inhibit the ECL reaction. In contrast to L75H CtrHb that was bound with cyanide prior to reduction (lane 4), the imidazole sample that was cleaned by passage through DEAE (L75H +Im/+DEAE, lane 3) only shows partial crosslinking. *Synechocystis* 6803 GlbN-A (lane 5) and L75H CtrHb with no exogenous ligand added were used as positive and negative controls, respectively. The film was exposed for 7 min.

References

[1] M. Milani, Y. Ouellet, H. Ouellet, M. Guertin, A. Boffi, G. Antonini, A. Bocedi, M. Mattu, M. Bolognesi, P. Ascenzi, Biochemistry 43 (2004) 5213-5221.

[2] M. Couture, M. Guertin, Eur. J. Biochem. 242 (1996) 779-787.